The high-energy antiproton-to-proton flux ratio with the PAMELA experiment

M. Bongi[*], O. Adriani[†*], G. C. Barbarino[‡§], G. A. Bazilevskaya[¶], R. Bellotti[‖], M. Boezio[††], E. A. Bogomolov[‡‡], L. Bonechi[†*], V. Bonvicini[††], S. Bottai[*], A. Bruno[‖**], F. Cafagna[‖], D. Campana[§], P. Carlson[xiii], M. Casolino[x], G. Castellini[xiv], M. P. De Pascale[x xii], G. De Rosa[§], N. De Simone[x xii], V. Di Felice[x xii], A. M. Galper[xi], L. Grishantseva[xi], P. Hofverberg[xiii], S. V. Koldashov[xi], S. Y. Krutkov[‡‡], A. N. Kvashnin[¶], A. Leonov[xi], V. Malvezzi[x], L. Marcelli[x], W. Menn[xv], V. V. Mikhailov[xi], E. Mocchiutti[††], G. Osteria[§], P. Papini[*], M. Pearce[xiii], P. Picozza[x xii], M. Ricci[xvi], S. B. Ricciarini[*], M. Simon[xv], R. Sparvoli[x xii], P. Spillantini[†*], Y. I. Stozhkov[¶], A. Vacchi[††], E. Vannuccini[*], G. Vasilyev[‡‡], S. A. Voronov[xi], Y. T. Yurkin[xi], G. Zampa[††], N. Zampa[††], and V. G. Zverev[xi]**

[*] *INFN, Sezione di Firenze, Via Sansone 1, I-50019 Sesto Fiorentino, Florence, Italy*
[†] *University of Florence, Department of Physics, Via Sansone 1, I-50019 Sesto Fiorentino, Florence, Italy*
[‡] *University of Naples "Federico II", Department of Physics, Via Cintia, I-80126 Naples, Italy*
[§] *INFN, Sezione di Napoli, Via Cintia, I-80126 Naples, Italy*
[¶] *Lebedev Physical Institute, Leninsky Prospekt 53, RU-119991 Moscow, Russia*
[‖] *University of Bari, Department of Physics, Via Amendola 173, I-70126 Bari, Italy*
[**] *INFN, Sezione di Bari, Via Amendola 173, I-70126 Bari, Italy*
[††] *INFN, Sezione di Trieste, Padriciano 99, I-34012 Trieste, Italy*
[‡‡] *Ioffe Physical Technical Institute, Polytekhnicheskaya 26, RU-194021 St. Petersburg, Russia*
[x] *INFN, Sezione di Roma "Tor Vergata", Via della Ricerca Scientifica 1, I-00133 Rome, Italy*
[xi] *Moscow Engineering and Physics Institute, Kashirskoe Shosse 31, RU-11540 Moscow, Russia*
[xii] *University of Rome "Tor Vergata", Department of Physics, Via della Ricerca Scientifica 1, I-00133 Rome, Italy*
[xiii] *KTH, Department of Physics AlbaNova University Centre, SE-10691 Stockholm, Sweden*
[xiv] *IFAC, Via Madonna del Piano 10, I-50019 Sesto Fiorentino, Florence, Italy*
[xv] *Universität Siegen, D-57068 Siegen, Germany*
[xvi] *INFN, Laboratori Nazionali di Frascati, Via Enrico Fermi 40, I-00044 Frascati, Italy*

***Abstract*. The PAMELA experiment is a satellite-borne apparatus designed to study charged particles in the cosmic radiation, with a particular focus on antiparticles. The detector is housed on the Resurs-DK1 satellite and it is taking data since June 2006. The main parts of the apparatus are a magnetic spectrometer, which is equipped with a silicon-microstrip tracking system and which is used to measure the rigidity and the charge of particles, and a silicon/tungsten electromagnetic calorimeter which provides particle identification. The results of the analysis of the antiproton-to-proton flux ratio between 1 and 100 GeV which employs the data collected in 500 days is presented here. A total of about 1000 antiprotons have been identified, including 100 above an energy of 20 GeV.**

***Keywords*: Satellite detector, antiproton-to-proton ratio, dark matter.**

I. Introduction

Antiprotons which are detected outside the Earth's atmosphere can be the result of interactions between energetic cosmic-ray protons and nuclei in the interstellar medium. This known mechanism is referred to as "secondary" production: other possible "primary" sources of galactic antiprotons could exist, such as the annihilation of dark matter particles [1], [2], or the evaporation of primordial black holes [3], [4]. Cosmic-ray antiproton experiments can provide useful data for studying production and transport properties of cosmic rays in the Galaxy, and they can also test the correctness of exotic production mechanisms. However, such detailed studies of the antiproton energy spectrum require measurements with good statistics over a large energy range.

Cosmic-ray antiprotons were first observed in pioneering experiments in the 1970s by Bogomolov *et al.* [5] and Golden *et al.* [6] using balloon-borne magnetic spectrometers. Bogomolov *et al.* observed 2 antiprotons in the kinetic energy range 2–5 GeV while Golden *et al.* observed 28 antiprotons in the range 5–12 GeV. Several other experiments followed, covering the kinetic energy range 0.2–50 GeV. More than 1000 antiprotons have been observed in the kinetic energy range 0.2–4 GeV by the BESS experiment [7] while the statistics at higher energies is very limited. The CAPRICE98 [8], HEAT [9], and MASS91 [10] balloon-borne experiments have observed a total of

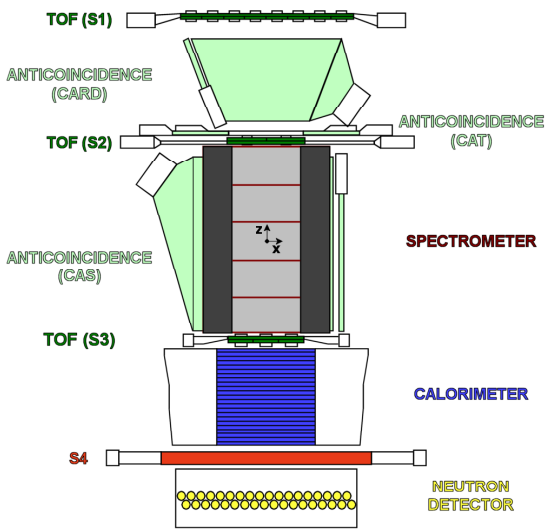

Fig. 1: Schematic drawing of the PAMELA detector showing the sensitive areas of the various sub-systems to scale, in a longitudinal section.

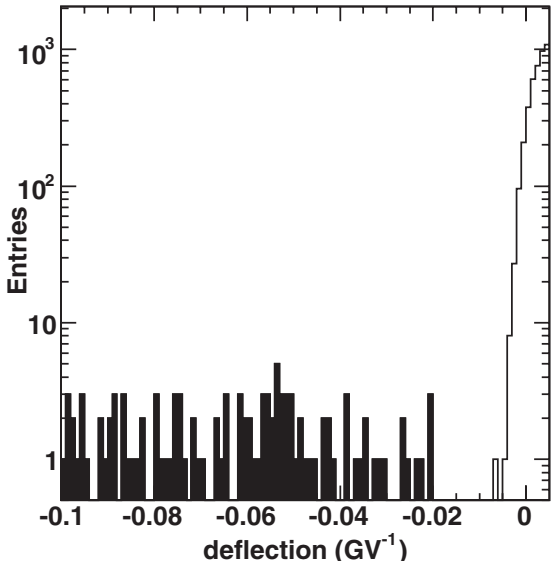

Fig. 2: Deflection distribution for down-going particles with a reconstructed MDR $\geq$ 850 GV which did not produce an electromagnetic shower in the calorimeter. The good separation between positive and negative particles can be seen, as well as the spillover of positively charged particles into the negative deflection region. The shaded part of the histogram corresponds to particles selected as antiprotons.

about 80 antiprotons above 5 GeV. However, only two cosmic-ray antiprotons with a kinetic energy above 30 GeV are reported [8].

II. The PAMELA detector

The PAMELA experiment [11] (a Payload for Antimatter Matter Exploration and Light-nuclei Astrophysics) has measured the antiproton-to-proton flux ratio up to 100 GeV obtaining a significant increase in the statistics, particularly at high energies [12].

The detector is located inside a pressurized container attached to the Russian Resurs-DK1 satellite and it is composed of several sub-systems (see Fig. 1): three double-layer planes of plastic scintillators form the time-of-flight system (ToF); a permanent magnet and a silicon-microstrip tracking system form the magnetic spectrometer; another set of plastic scintillators are arranged around and on top of the magnet and are used as an anticoincidence system; an electromagnetic imaging calorimeter is composed of silicon detectors and tungsten absorbers; a shower-tail catcher scintillator (S4) is placed under the calorimeter; a ^{3}He neutron detector at the bottom of the apparatus completes the detector.

III. Data analysis

Some details of the analysis of data acquired from the middle of July 2006 to the end of February 2008 are reported here. This period corresponds to a total acquisition time of about 500 days, and to more than 10^9 triggers. Further analysis is progress in order to increase the statistics and the energy range of the measured antiproton-to-proton flux ratio: results will be presented at this Conference and in future publications.

After the event reconstruction, particles are preselected by requiring their rigidity to exceeded the vertical geomagnetic cut-off (which is estimated on the basis of the satellite position) by a factor of 1.3. Albedo particles are rejected using time-of-flight information: the ToF resolution of 300 ps ensures that no contamination from upward-going particles remains in the selected sample. The ionization losses in the ToF scintillators and in the silicon tracker planes are used to select minimum-ionizing particles with charge Z=1, and multi-particle events are rejected by requiring no spurious signals in the time-of-flight and anticoincidence scintillators above the tracking system. The sign of the charge and the rigidity are determined by the deflection of the particle inside the magnetic spectrometer, while the properties of the energy deposit and of the interaction topology in the calorimeter provides identification and hadron/lepton separation. The analysis technique was validated using Monte Carlo simulations, which have been tuned using data from several beam tests.

The most crucial point of the analysis consists in the selection of the rare antiproton component among the much higher number of protons (which are about 10^4 times more abundant). In particular, because of the finite spectrometer resolution, which corresponds to a maximum detectible rigidity (MDR) exceeding 1 TV, high-rigidity protons may be assigned the wrong sign of curvature inside the magnetic field of the spectrometer. In addition, protons can scatter inside the material they find while crossing the detector and they can thus

mimic the trajectory of negatively-charged particles. The design of the tracking system is optimized in order to minimize this kind of background, as the silicon sensor planes have been built without any additional material on the path of particles inside the magnet cavity. The "spillover" of particles with the wrong sign of charge can be eliminated by imposing a set of strict selection criteria on the quality of the fitted tracks. Tracks are required to include at least 4 position measurements along the x direction on the silicon sensors (which is the main bending direction inside the almost uniform magnetic field), and at least 3 along the y direction. An acceptable value for the χ^2 from the fit of the trajectory is also requested. In order to exclude spillover protons from the antiproton sample, quality check are performed on the hits associated to a track (e.g., no accompanying hits due to emission of delta rays, which could result in a wrong position measurement), and an MDR 10 times higher than the reconstructed rigidity of the particle is required. The MDR for each event is estimated during the fitting procedure on the basis of the geometric characteristics of the track and of the spatial resolution associated to the hits. The distribution of the deflection (1/rigidity) as reconstructed by the track fitting procedure for positively- and negatively-charged down-going particles which have a MDR $\geq$ 850 GV and which did not produce an electromagnetic shower in the calorimeter is shown in Fig. 2. The good separation between negatively charged particles and the spillover protons coming from the positive-deflection region is evident.

The rejection of electrons is done by means of the calorimeter. Its good longitudinal and transverse segmentation combined with dE/dx measurements from the individual silicon strips allow electromagnetic showers to be identified with very high accuracy. For the identification of antiprotons, topological criteria have been developed [13] on the basis of the analysis of beam tests and simulations involving both electrons and antiprotons. An example of a calorimeter topological variable is shown in Fig. 3: the plots show the distribution of the energy density in the core of the shower produced by the particle weighted by the depth inside the calorimeter (Q_{core}/N_{core}) for negative and positive particles. The peak of the distribution in the case of the positive sample, which is amply dominated by protons, is located around $Q_{core}/N_{core} = 1.25$; the corresponding peak in the negative sample represents antiprotons, while the distribution for electrons is located at higher values of the variable. The resulting electron contamination has been estimated to be negligible in the whole energy range of interest. The different interaction cross-sections for protons and antiprotons have been taken into account estimating the calorimeter selection efficiencies as a function of momentum for both species. These efficiencies were studied using both simulated antiprotons and protons, and proton samples selected from the flight data, and they have been used to rescale

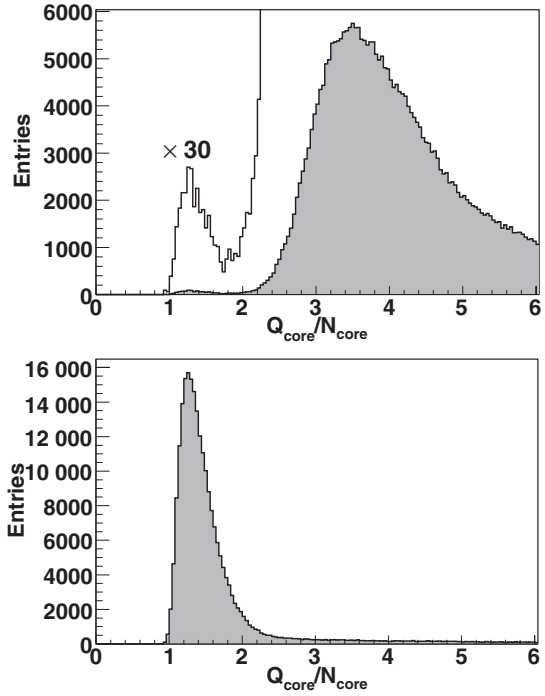

Fig. 3: Distribution of the energy density in the shower core weighted by the depth in the calorimeter (Q_{core}/N_{core}) for negative (upper plot) and positive (lower plot) particles. In order to show better the left peak in the case of negative particles, the same distribution is also reported with the vertical scale multiplied by a factor 30 (white histogram).

the number of selected antiprotons and protons. Possible contamination from charged pions produced by cosmic-ray interactions with the PAMELA detectors or with the pressure vessel has been studied using both simulated and flight data. For rigidity lower than 1 GV pions can be identified and rejected using the β (velocity) measured by the ToF system and the calorimeter information; for higher rigidities the residual contamination is estimated to be less than 5% above 2 GV, decreasing to less than 1% above 5 GV.

The number of protons and antiprotons which survived the data selection have been corrected for the calorimeter selection efficiencies and for the loss of particles inside the instrument itself. The antiproton-to-proton flux ratio which has been been measured by the PAMELA experiment is shown in Fig. 4 where it is compared with theoretical calculations which assume pure secondary production of antiprotons during the propagation of cosmic rays in the Galaxy, and in Fig. 5 where data from other recent experiments is also shown. The reported errors are statistical only while the contamination, which is estimated to be less than a few percent of the signal, has not been subtracted from the results and should be considered as a systematic uncertainty.

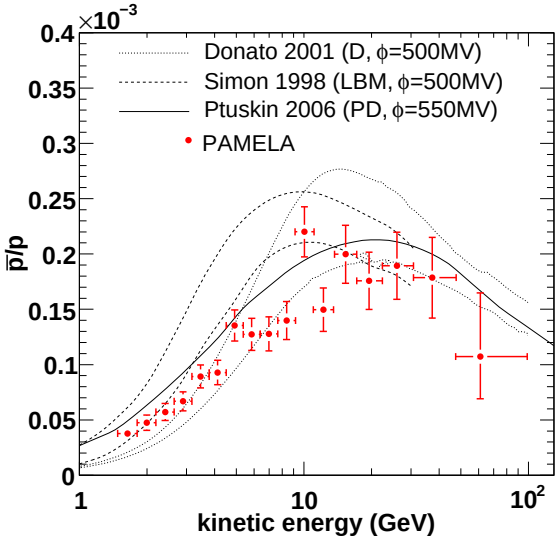

Fig. 4: The antiproton-to-proton flux ratio measured by the PAMELA experiment compared with theoretical calculations for a pure secondary production of antiprotons during the propagation of cosmic rays in the Galaxy. The dotted lines show the upper and lower limits from Donato *et al.* [14] for a Diffusion model with reacceleration, while the dashed lines show the limits calculated by Simon *et al.* [15] for the standard Leaky Box Model. The solid line shows the calculation by Ptukin *et al.* [16] for the case of a Plain Diffusion model. The curves were obtained using an appropriate solar modulation parameter (indicated as ϕ) for the PAMELA data taking period.

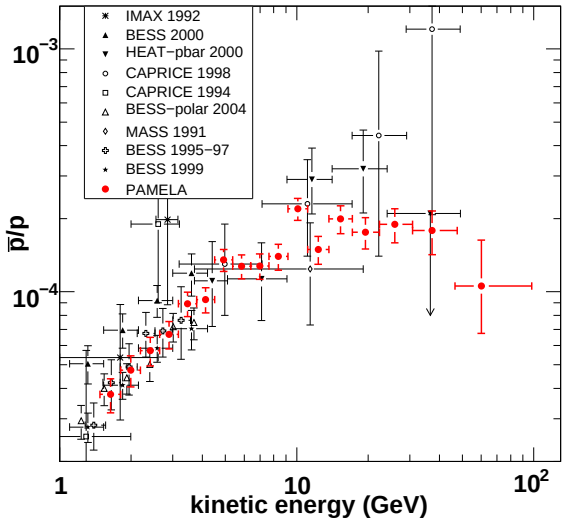

Fig. 5: The antiproton-to-proton flux ratio measured by the PAMELA experiment compared with other recent measurements [8], [9], [10], [17], [18], [19], [20].

IV. Conclusions

The PAMELA experiment has measured the antiproton-to-proton flux ratio over the most extended energy range ever achieved and has improved the existing statistics at high energies by an order of magnitude. The measured ratio increases smoothly from about 4×10^{-5} at a kinetic energy of about 1 GeV and levels off at about 1×10^{-4} for energies above 10 GeV. The results are sufficiently precise to place tight constraints on parameters relevant for secondary production calculations and they provide important test criteria for cosmic-ray propagation models. The high-energy data above 10 GeV can place important limits on contributions from exotic sources, in particular on annihilation of dark-matter particles, as the antiproton-to-proton flux ratio would change according to different values of the mass of the dark-matter particles, their annihilation cross section, and structure in the density profile (boost factor).

References

[1] G. Jungman, M. Kamionkowski, and K. Griest, Phys. Rep. **267**, 195 (1996).
[2] G. Bertone, D. Hooper, and J. Silk, Phys. Rep. **405**, 279 (2005).
[3] S. Hawking, Nature (London) **248**, 30 (1974).
[4] P. Kiraly *et al.* , Nature (London) **293**, 120 (1981).
[5] E. A. Bogomolov *et al.* , *Proceeedings of the 16th International Cosmic Ray Conference (Kyoto)* (Institute for Cosmic Ray Research, University of Tokyo, Tokyo, Japan, 1979), Vol. 1, p. 330.
[6] R. L. Golden *et al.* , Phys. Rev. Lett. **43**, 1196 (1979).
[7] A. Yamamoto *et al.* , Nucl. Phys. B, Proc. Suppl. **166**, 62 (2007).
[8] M. Boezio *et al.* , Astrophys. J. **561**, 787 (2001).
[9] A. S. Beach *et al.* , Phys. Rev. Lett. **87**, 271101 (2001).
[10] M. Hof *et al.* , Astrophys. J. Lett. **467**, L33 (1996).
[11] P. Picozza *et al.* , Astropart. Phys. **27**, 296 (2007).
[12] O. Adriani *et al.* , Phys. Rev. Lett. **102**, 051101 (2009).
[13] M. Boezio *et al.* , Astropart. Phys. **26**, 111 (2006).
[14] F. Donato *et al.* , Astrophys. J. **563**, 172 (2001).
[15] M. Simon, A. Molnar, and S. Roesler, Astrophys. J. **499**, 250 (1998).
[16] V. S. Ptuskin *et al.* , Astrophys. J. **642**, 902 (2006).
[17] J. Mitchell *et al.* , Phys. Rev. Lett. **76**, 3057 (1996).
[18] M. Boezio *et al.* , Astrophys. J. **487**, 415 (1997).
[19] Y. Asaoka *et al.* , Phys. Rev. Lett. **88**, 051101 (2002).
[20] T. Hams *et al.* , *Proceedings of the 30th International Cosmic Ray Conference (Merida)* (Universidad Nacional Autonóma de México, Mexico City, Mexico, 2008), Vol. 2, p. 67.